

Human ortholog of *Drosophila* Melted impedes SMAD2 release from TGF- β receptor I to inhibit TGF- β signaling

Premalatha Shathasivam^{a,b,c}, Alexandra Kollara^{a,c}, Maurice J. Ringuelette^d, Carl Virtanen^e, Jeffrey L. Wrana^{a,f}, and Theodore J. Brown^{a,b,c,1}

^aLunenfeld-Tanenbaum Research Institute at Mount Sinai Hospital, Toronto, ON, Canada M5T 3H7; Departments of ^bPhysiology, ^cObstetrics and Gynaecology, ^dCell and Systems Biology, and ^eMolecular Genetics, University of Toronto, Toronto, ON, Canada M5S 3G5; and ^fPrincess Margaret Cancer Centre, University Health Network, Toronto, ON, Canada M5G 1L7

Edited by Igor B. Dawid, The Eunice Kennedy Shriver National Institute of Child Health and Human Development, National Institutes of Health, Bethesda, MD, and approved May 5, 2015 (received for review March 11, 2015)

Drosophila melted encodes a pleckstrin homology (PH) domain-containing protein that enables normal tissue growth, metabolism, and photoreceptor differentiation by modulating Forkhead box O (FOXO), target of rapamycin, and Hippo signaling pathways. Ventricular zone expressed PH domain-containing 1 (VEPH1) is the mammalian ortholog of *melted*, and although it exhibits tissue-restricted expression during mouse development and is potentially amplified in several human cancers, little is known of its function. Here we explore the impact of VEPH1 expression in ovarian cancer cells by gene-expression profiling. In cells with elevated VEPH1 expression, transcriptional programs associated with metabolism and FOXO and Hippo signaling were affected, analogous to what has been reported for Melted. We also observed altered regulation of multiple transforming growth factor- β (TGF- β) target genes. Global profiling revealed that elevated VEPH1 expression suppressed TGF- β -induced transcriptional responses. This inhibitory effect was verified on selected TGF- β target genes and by reporter gene assays in multiple cell lines. We further demonstrated that VEPH1 interacts with TGF- β receptor I (T β RI) and inhibits nuclear accumulation of activated Sma- and Mad-related protein 2 (SMAD2). We identified two T β RI-interacting regions (TIRs) with opposing effects on TGF- β signaling. TIR1, located at the N terminus, inhibits canonical TGF- β signaling and promotes SMAD2 retention at T β RI, similar to full-length VEPH1. In contrast, TIR2, located at the C-terminal region encompassing the PH domain, decreases SMAD2 retention at T β RI and enhances TGF- β signaling. Our studies indicate that VEPH1 inhibits TGF- β signaling by impeding the release of activated SMAD2 from T β RI and may modulate TGF- β signaling during development and cancer initiation or progression.

VEPH1 | TGF- β | SMAD2/3 | Melted | ALK5

Ventricular zone expressed pleckstrin homology domain-containing 1 (*Veph1*) was initially identified as a novel gene encoding an 833-amino-acid protein expressed in the developing murine central nervous system (1). In the adult mouse, *Veph1* expression is restricted to the eye and kidney. Although the function of *Veph1* in mammals is unknown, the *Drosophila* ortholog *melted* impacts tissue growth and metabolism (2). Disruption of *melted* in *Drosophila* results in a 10% reduction in adult size, which is rescued by transgenic expression of *melted* or human *VEPH1*. Mutant flies have reduced fat (triglyceride) content attributable to decreased Melted, specifically within the fat body. Comparison of gene expression profiles of fat bodies from wild-type (WT) and Melted-deficient flies identified altered expression of genes involved in metabolism, protein degradation, and immune response. Melted inhibits Forkhead box O (FOXO) and promotes target of rapamycin (TOR) signaling—pathways involved in regulating metabolism and tissue growth—by localizing FOXO and Tsc1/Tsc2 complexes to the plasma cell membrane. Melted has also been shown to regulate R8 color photoreceptor differentiation by opposing the expression of *warts*, a tumor suppressor and key component of the Hippo signaling pathway (2–5).

The gene locus encompassing human *VEPH1*, 3q24-25, lies within a region frequently amplified in ovarian cancer (6, 7). Tan et al. (8) found that this locus was also amplified in 7 of 12 epithelial ovarian cancer cell lines. A gene copy number analysis of 68 primary tumors by Ramakrishna et al. (9) identified frequent (>40%) *VEPH1* gene amplification that correlated with transcript levels. We determined the impact of VEPH1 on gene expression in an ovarian cancer cell line using a whole-genome expression array. The results indicate a gene-expression profile that is partially consistent with that reported for Melted and raises the possibility that VEPH1 may modulate TGF- β signaling.

TGF- β is a pleiotropic cytokine that regulates tissue development, repair, remodeling, and homeostasis by affecting cell proliferation, differentiation, survival, and migration. TGF- β signals by inducing the formation of a heterotetrameric complex of type II (T β RII) and type I (T β RI; ALK5) serine/threonine kinase transmembrane receptors (10). Ligand-bound, constitutively active T β RII phosphorylates T β RI, resulting in T β RI association with and C-terminal phosphorylation of Sma- and Mad-related protein 2 (SMAD2) and/or SMAD3 (SMAD2/3) (11). In the canonical TGF- β signaling pathway, phosphorylated SMAD2/3 rapidly dissociates from T β RI and oligomerizes with SMAD4. The SMAD2/3–SMAD4 complex then accumulates in the nucleus

Significance

Ventricular zone expressed pleckstrin homology domain-containing 1 (*VEPH1*) is among genes on chromosome 3q24-26, a region amplified in several cancers. Although little is known of mammalian VEPH1, its *Drosophila* ortholog, Melted, is involved in neural and eye development, metabolism, and size determination through effects on Forkhead box O, target of rapamycin, and Hippo signaling. We show that VEPH1 expression affects similar gene categories as Melted and potentially inhibits transforming growth factor- β (TGF- β) signaling. VEPH1 interacts with TGF- β type I receptor (T β RI) and inhibits dissociation of activated Sma- and Mad-related protein 2 from T β RI, resulting in impaired TGF- β signaling. TGF- β acts initially as a tumor suppressor through its cytostatic activity, but subsequently promotes tumor progression. These findings suggest that VEPH1 could affect TGF- β activity during cancer development/progression.

Author contributions: P.S., A.K., M.J.R., J.L.W., and T.J.B. designed research; P.S. and A.K. performed research; P.S., J.L.W., and T.J.B. contributed new reagents/analytic tools; P.S., A.K., C.V., and T.J.B. analyzed data; and P.S., A.K., M.J.R., J.L.W., and T.J.B. wrote the paper.

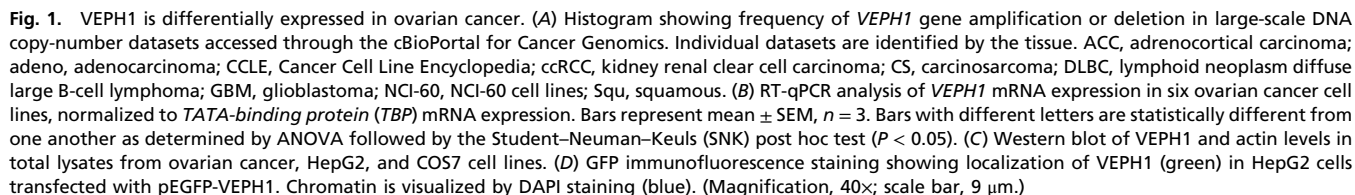
The authors declare no conflict of interest.

This article is a PNAS Direct Submission.

Data deposition: The microarray data reported in this paper have been deposited in the Gene Expression Omnibus (GEO) database, www.ncbi.nlm.nih.gov/geo (accession no. GSE67765).

¹To whom correspondence should be addressed. Email: brown@lunenfeld.ca.

This article contains supporting information online at www.pnas.org/lookup/suppl/doi:10.1073/pnas.1504671112/-DCSupplemental.



In this study, we demonstrate that VEPH1 suppresses TGF- β signaling by impeding the nuclear accumulation of activated SMAD2. Our data indicate that this effect is mediated by VEPH1 interaction with T β RI, which suppresses dissociation of phosphorylated SMAD2 from the TGF- β receptor complex. These findings highlight an additional pathway that may be affected by Melted and suggest that modulation of TGF- β signaling by VEPH1 may play a role in the initiation or progression of a subset of ovarian cancers.

Previous studies indicate that Melted affects FOXO and Hippo signaling pathways in *Drosophila*. Moreover, putative FOXO and 14-3-3 protein-binding motifs are conserved between Melted and human VEPH1 [Eukaryotic Linear Motif (ELM) (32)]. In the present study, DAVID analysis identified the Wnt signaling pathway as possibly affected by VEPH1 ($P = 0.069$). VEPH1 altered the expression of multiple genes encoding Wnt signaling components (Table S2). TGF- β has been implicated in

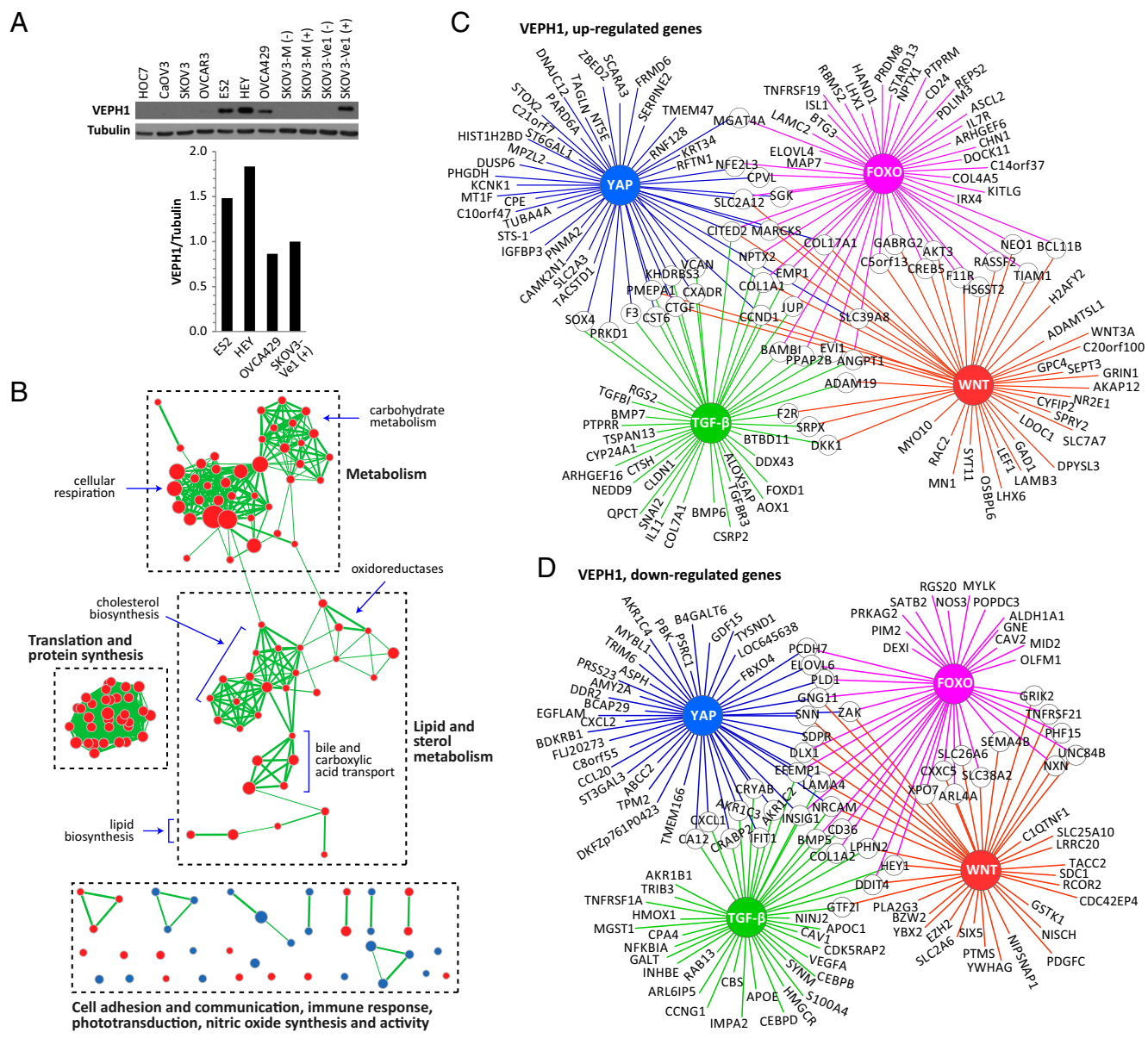


Fig. 2. Genome-wide gene-expression profiling indicates that VEPH1 expression affects multiple cell-signaling pathways and processes. (A) Western blot using an anti-VEPH1 antibody showing VEPH1 expression in stably transfected SKOV3-Ve1 cells and ovarian cancer cell lines. Histogram shows VEPH1 levels normalized to tubulin. + or – indicates presence or absence of CdCl₂ pretreatment, respectively. (B) Cytoscape visualization of cellular processes altered by VEPH1 expression as determined by GSEA of genes differentially expressed between SKOV3-M and -Ve1 cells. Three major cluster groups were identified along with several noncluster processes (Fig. S1). Each node represents a set of genes involved in the identified cell process, with the size of the node reflecting the number of genes affected by VEPH1. Red represents enrichment in SKOV3-M cells, and blue represents enrichment in SKOV3-Ve1 cells. Edges indicate sharing of affected gene members between individual nodes, with the thickness of the edge reflecting the number of genes shared. (C and D) Cytoscape visualization of FOXO, Hippo (YAP), Wnt, and TGF- β -regulated target genes altered by VEPH1 expression greater than or equal to twofold. (C) VEPH1, up-regulated genes. (D) VEPH1, down-regulated genes.

regulation of several of the VEPH1-affected KEGG pathways, including focal adhesion, neurotrophin signaling, and amyotrophic lateral sclerosis (33–36). A high-throughput screen by Barrios-Rodiles et al. (37) identified the PH-domain-containing region of murine Veph1 as a potential interactor of T β RI. We therefore determined whether downstream targets of these four signaling pathways are altered in SKOV3-Ve1 cells relative to SKOV3-M cells. Comparison of probe sets altered ≥ 1.5 -fold due to VEPH1 expression to compiled lists of known or putative target genes revealed that expression of 173 FOXO, 274 Hippo [Yes-associated protein (YAP)], 170 Wnt, and 133 TGF- β target genes was affected by VEPH1 (Tables S3 and S4). Fig. 2 C and D illustrate those target genes up- and down-regulated, respectively,

by VEPH1 expression. Multiple genes are downstream targets of two or more of the highlighted signaling pathways. This analysis demonstrates that VEPH1 likely affects FOXO and Hippo signaling as reported for Melted and additionally indicates that Wnt and TGF- β signaling may be modulated by VEPH1.

VEPH1 Has a Global Negative Impact on TGF- β Signaling. To further determine whether VEPH1 modulates TGF- β signaling, we compared gene-expression profiles of SKOV3-Ve1 and -M cells treated with or without TGF- β . Treatment of SKOV3-M cells with TGF- β for 3 h resulted in altered expression of 454 probe sets. In contrast, only 283 probe sets were modulated by TGF- β in SKOV3-Ve1 cells. Approximately 20% of probe sets (92 of 454)

modulated by TGF- β in SKOV3-M cells were also altered by TGF- β in SKOV3-Ve1 cells (Fig. 3A). Applying a TGF- β -induced 1.5-fold change or greater cutoff to these gene lists indicates that TGF- β altered 65 probe sets in SKOV3-M cells, whereas only 9 were affected by TGF- β in SKOV3-Ve1 cells (Fig. 3B and Tables S5 and S6). Of these nine, only one was modulated by TGF- β in SKOV3-Ve1 cells that was not affected in SKOV3-M cells. Furthermore, the impact of TGF- β is diminished in the presence of VEPH1 in seven of the eight probe sets common to both cell lines. Overall, these findings indicate a global inhibition of TGF- β -induced gene responses by VEPH1 expression.

To verify the impact of VEPH1 on TGF- β -dependent target gene expression observed in the gene expression profile study, we selected three well-established TGF- β target genes that exhibited diminished TGF- β stimulation in the presence of VEPH1 relative to control transfected cells: plasminogen activator inhibitor 1 (*PAI-1*), *SMAD7*, and inhibitor of differentiation 1 (*ID1*). Whereas TGF- β treatment in SKOV3-M cells resulted in a 4.6- and 2.4-fold up-regulation of *PAI-1* and *SMAD7* transcripts, respectively, this up-regulation was reduced to 2.8- and 1.9-fold, respectively, in SKOV3-Ve1 cells (Fig. 3C). The impact of VEPH1 on TGF- β -induced *ID1* expression was examined by Western blot analysis. The highest levels of *ID1* protein were observed 1.5 h after TGF- β treatment in both SKOV3-Ve1 and -M cells (Fig. 3D). However, VEPH1 expression decreased TGF- β -induced *ID1* protein levels at all time points examined (SKOV3-Ve1 vs. SKOV3-M).

VEPH1 inhibition of TGF- β -induced *SMAD7* expression was further demonstrated by knockdown studies in HEY cells, which express high levels of endogenous VEPH1 (Fig. 1B and C). Four individual VEPH1-targeting siRNAs were screened, with siVEPH1 nos. 1 and 2 providing the highest levels of knockdown (Fig. 3E). TGF- β increased *SMAD7* mRNA, with the highest transcript levels observed 1 h after treatment (Fig. 3F). Silencing VEPH1 expression with siVEPH1 no. 1 or 2 increased *SMAD7* transcripts relative to TGF- β -treated controls (Fig. 3F and G). Together, these findings demonstrate that VEPH1 negatively modulates TGF- β signaling.

VEPH1 Inhibits SMAD2- and SMAD3-Dependent TGF- β Signaling. To determine whether VEPH1 affects canonical SMAD2/3-dependent TGF- β signaling, we examined the impact of ectopic human VEPH1 expression on TGF- β -dependent transcriptional responses in SKOV3-M, -Ve, COS7, and HepG2 cells using SMAD2- and SMAD3-dependent reporters [pARE- and pSBE4-luciferase (38, 39), respectively]. In the absence of CdCl₂ treatment, SKOV3-Ve1 clones express detectable VEPH1 levels, whereas SKOV3-Ve2 clones express little or no VEPH1 (Fig. 4A and B, Westerns). In SKOV3-M cells, TGF- β increased pARE- and pSBE4-luciferase 4.4- and 3.7-fold, respectively, whereas in SKOV3-Ve1 cells, TGF- β induction of pARE-luciferase was blocked, and induction of pSBE4-luciferase was decreased by 50% (Fig. 4A). A slight decrease in pARE-luciferase activity in the absence of TGF- β was observed in SKOV3-Ve1 cells, consistent with an impact on autocrine TGF- β signaling in SKOV3 cells (Fig. S2). Induction of VEPH1 expression in SKOV3-Ve2 cells with increasing amounts of CdCl₂ resulted in a dose-dependent decrease in TGF- β -induced pARE- and pSBE4-luciferase activity (Fig. 4B). To determine whether this negative impact of VEPH1 extends to other cell types, we performed parallel experiments in transiently transfected COS7 and HepG2 cells. TGF- β stimulation resulted in 8.5- and 145-fold activation of SMAD2-dependent signaling in COS7 and HepG2 cells, respectively, and ectopic VEPH1 expression inhibited this activation in a dose-dependent manner in both cell lines (Fig. 4C and D). At the highest levels of VEPH1, SMAD2-dependent signaling was decreased by >70%. A marked reduction of up to 50% in SMAD3-dependent signaling by VEPH1 was also observed in HepG2 cells (Fig. 4D). Overall, these data demonstrate that VEPH1 attenuates both SMAD2- and SMAD3-dependent TGF- β signaling.

VEPH1 Inhibits SMAD2 Nuclear Accumulation and Promotes SMAD2 Retention at T β RI. To determine the mechanism by which VEPH1 inhibits TGF- β signaling, we first examined the impact of VEPH1

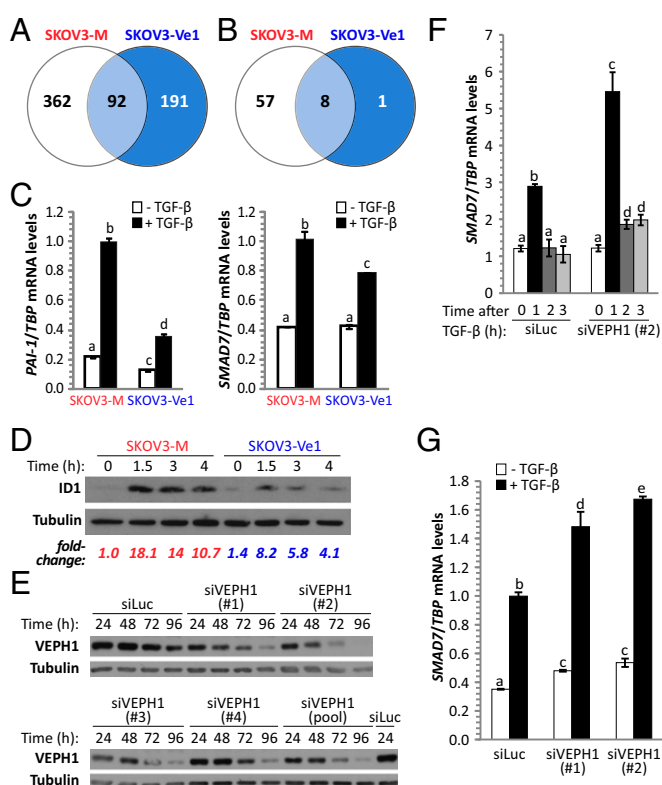


Fig. 3. VEPH1 negatively regulates activation of TGF- β -induced target genes. (A) Venn diagram showing total number of probe sets significantly altered by TGF- β in SKOV3-Ve1 and -M cells. (B) Venn diagram showing probe sets significantly altered ≥ 1.5 -fold by TGF- β in SKOV3-Ve1 and -M cells. (C) VEPH1 inhibits TGF- β activation of *PAI-1* and *SMAD7* in SKOV3-Ve1 cells, as determined by RT-qPCR. RNA was extracted from CdCl₂-induced SKOV3-Ve1 and -M cells treated with or without 25 pM TGF- β for 3 h. mRNA levels were normalized to *TBP* expression. (D) Western blot showing VEPH1 inhibition of TGF- β -induced *ID1* protein expression in SKOV3-Ve1 cells. Total protein was extracted from cells treated with 25 pM TGF- β for the indicated times. Tubulin expression is shown as a loading control. Fold changes shown are relative to SKOV3-M cells in the absence of TGF- β . (E) VEPH1 knockdown efficiency was determined for a pool of four VEPH1 targeting siRNAs or each individually in HEY cells. HEY cells were transfected with luciferase targeting siRNA (siLuc) as a control. Protein lysates were collected at 24, 48, 72, and 96 h after siRNA transfection and subjected to immunoblotting for VEPH1. (F and G) VEPH1 knockdown enhances TGF- β -induced *SMAD7* gene expression in HEY cells, as determined by RT-qPCR. HEY cells were transfected with siLuc or siVEPH1 (no. 1 or 2) 96 h (F) or 48 h (G) before treatment with or without 100 pM TGF- β . RNA was extracted after TGF- β treatment for the indicated times (F) or 1 h after treatment (G). *SMAD7* mRNA levels were normalized to *TBP* expression. Bars represent mean \pm SEM, $n = 3$. Bars with different letters are statistically different from one another as determined by ANOVA followed by SNK post hoc test ($P < 0.05$).

expression on SMAD2/3 nuclear accumulation. Cytoplasmic and nuclear protein fractions were isolated from SKOV3-Ve1 and -M cells treated with or without TGF- β . As expected, TGF- β treatment decreased cytoplasmic and increased nuclear SMAD2 levels in the absence of VEPH1 (Fig. 5A). VEPH1 expression reduced TGF- β -induced nuclear SMAD2 accumulation at all time points examined. This reduction was also evident by immunofluorescence (Fig. S3). Knockdown of endogenous VEPH1 expression in ES2 cells resulted in increased SMAD2 and SMAD3 nuclear accumulation following TGF- β treatment (Fig. 5B). Time course analysis of TGF- β -induced phospho-SMAD2 levels indicated that VEPH1 does not impact C-terminal phosphorylation of SMAD2 (Fig. 5C and Fig. S4). Thus, the decreased nuclear accumulation of SMAD2 in the presence of VEPH1 is not a result of reduced ability of T β RI to phosphorylate SMAD2.

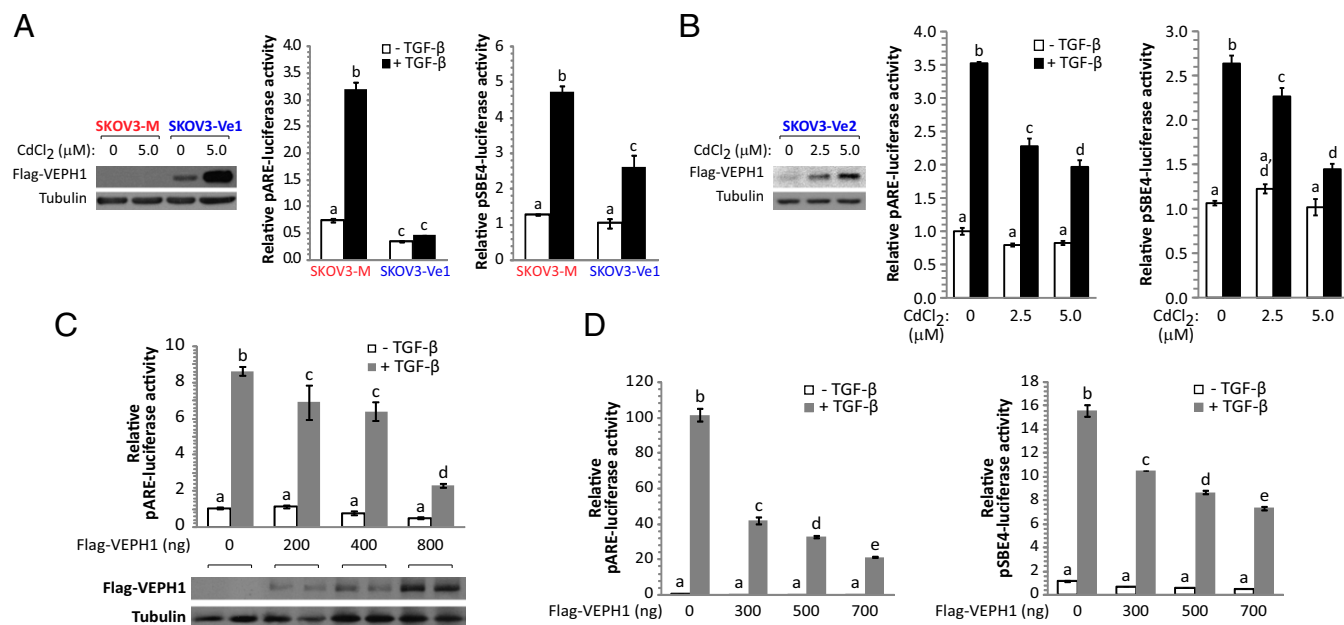


Fig. 4. VEPH1 inhibits SMAD2- and SMAD3-dependent TGF- β signaling. (A) CdCl₂-induced SKOV3-Ve1 cells have diminished SMAD2-dependent (pARE-luciferase) and SMAD3-dependent (pSBE4-luciferase) TGF- β signaling relative to SKOV3-M cells. (B) VEPH1 expression decreases TGF- β -dependent activation of both SMAD2- and SMAD3-dependent reporters in a dose-dependent manner in SKOV3-Ve2 cells. Cells in A and B were treated for 24 h with or without 25 pM TGF- β 24 h after reporter transfection. CdCl₂ induction of VEPH1 expression in SKOV3-Ve1 (A, Left) and SKOV3-Ve2 (B, Left) cells was confirmed by immunoblotting with Flag antibody. (C and D) Increased expression of VEPH1 inhibits SMAD2- and SMAD3-dependent TGF- β signaling in COS7 or HepG2 cells. COS7 (C) and HepG2 (D) cells were transiently transfected with empty vector or increasing amounts of Flag-VEPH1 and either a SMAD2-dependent (C and D) or SMAD3-dependent (D) reporter. Transfected cells were treated with or without 100 pM TGF- β for 24 h. Immunoblotting with anti-Flag antibody in C shows VEPH1 protein levels in COS7 cells transfected with increasing amounts of Flag-VEPH1. For all reporter assays, firefly luciferase activity was normalized to either β -galactosidase or Renilla luciferase (RL) activity. For pARE-luciferase assays, cells were cotransfected with a FoxH1 expression construct. Bars represent mean \pm SEM, $n = 3$. Bars with different letters are statistically different from one another as determined by ANOVA followed by SNK post hoc test ($P < 0.05$).

To identify how VEPH1 antagonizes SMAD2 nuclear accumulation, we analyzed the interaction of VEPH1 with T β RI and the impact of VEPH1 on SMAD2-T β RI association. Endogenous T β RI coprecipitated with both endogenous VEPH1 in HEY and Flag-tagged VEPH1 in SKOV3-Ve1 cells independent of TGF- β stimulation (Fig. 6A and B). VEPH1 impact on SMAD2-T β RI association was examined in both SKOV3 and HepG2 cells stably expressing CdCl₂-inducible Flag-VEPH1 (SKOV3- and HepG2-Ve1) or mock transfected (SKOV3- and HepG2-M) cells. In the absence of VEPH1, an interaction between T β RI and SMAD2 was detected in TGF- β -treated HepG2-M cells (Fig. 6C), which is consistent with TGF- β -induced transient recruitment of SMAD2 to T β RI. This interaction was not detected in SKOV3-M cells (Fig. 6B), likely due to the lower level of TGF- β sensitivity of these cells. In the presence of VEPH1, increased SMAD2 coprecipitation with T β RI was observed independent of TGF- β treatment in both SKOV3- and HepG2-Ve1 cells (Fig. 6B and C), indicating that VEPH1 recruits and retains SMAD2 at T β RI independent of T β RI activation by TGF- β .

Semiquantitative luminescence-based immunoprecipitation assay (LUMIER) (37) was used to quantify the impact of VEPH1 on the transient SMAD2-T β RI interaction. HEK293T human embryonic kidney cells were cotransfected with WT or constitutively active (TD) T β RI and Renilla luciferase (RL)-tagged SMAD2 expression constructs, with or without VEPH1. Total protein extracts were immunoprecipitated with an anti-T β RI antibody, and immunoprecipitates were assessed for RL activity. In the absence of VEPH1, an interaction between RL-SMAD2 and T β RI(TD) was observed (Fig. 6D), consistent with previous reports (37). As expected, little or no interaction was found between RL-SMAD2 and T β RI(WT). A VEPH1-induced dose-dependent increase in RL-SMAD2 interaction with T β RI(TD) was observed (Fig. 6D). A RL-SMAD2 interaction with T β RI(WT)

was also observed in the presence of VEPH1, consistent with our analysis of endogenous interactions in SKOV3- and HepG2-Ve1 cells (Fig. 6B and C). The SMAD2 retained at T β RI in the presence of VEPH1 is phosphorylated at the C terminus as shown in HEK293T cells (Fig. 6E). In the absence of VEPH1, association of phospho-SMAD2 with T β RI could not be detected, consistent with phosphorylation-induced release of SMAD2 from the receptor. The combined data demonstrate that VEPH1 impedes release of activated SMAD2 from T β RI.

Modulation of TGF- β Signaling by VEPH1 Is Dependent upon Its Interaction with T β RI. To further investigate the relationship between VEPH1-induced retention of SMAD2 at T β RI with its inhibitory effects on TGF- β signaling, we generated Flag-tagged VEPH1 deletion constructs (Fig. 7A) and examined their interaction with T β RI. VEPH1 deletion constructs lacking amino acids 661–833 (Δ 661) or 320–833 (Δ 320) both interacted with T β RI, as did a construct consisting of only the C-terminal PH-domain-containing region (662 Δ) (Fig. 7B). These findings thus indicate two T β RI-interacting regions (TIRs) on VEPH1: TIR-1, located within the first 319 amino acids of the N-terminal region; and TIR-2, located within the 171 C-terminal amino acids containing the PH domain. Interestingly, expression of VEPH1 fragments possessing TIR-1 inhibited TGF- β induction of pARE-luciferase similar to full-length VEPH1, whereas TIR-2 (662 Δ) enhanced TGF- β responsiveness (Fig. 7C). The enhancing effect of TIR-2 was also observed in HEY cells, in which expression of full-length VEPH1 only slightly inhibited TGF- β signaling (Fig. 7D), likely due to high levels of endogenous VEPH1.

To delineate the sequences within TIR-1 responsible for the interaction with T β RI and inhibition of TGF- β signaling, we generated deletion constructs consisting of amino acids 1–90 (Δ 91), 91–200 (90 Δ - Δ 201), or 201–319 (200 Δ - Δ 320) (Fig. 7A). The strongest interaction with T β RI was observed with 200 Δ - Δ 320,

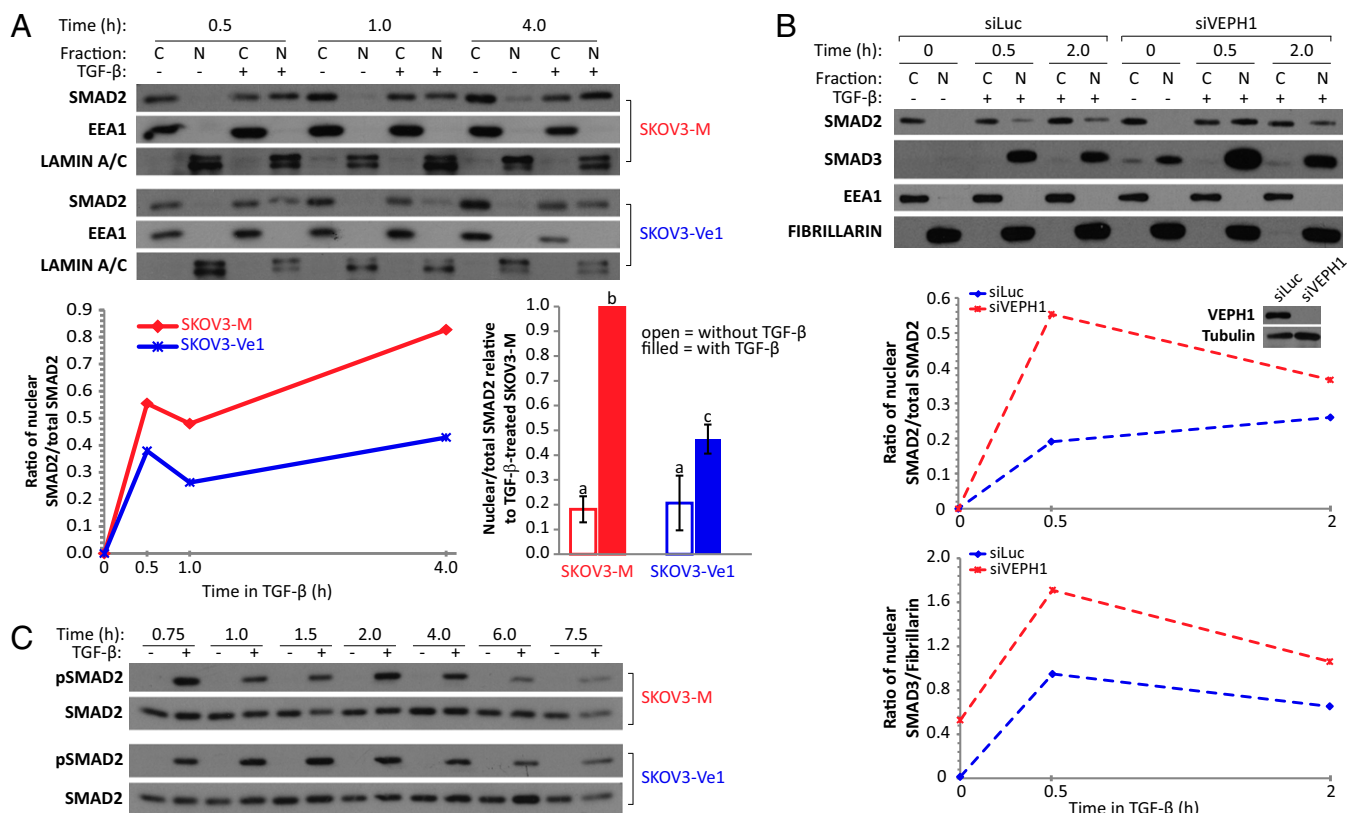


Fig. 5. VEPH1 impedes SMAD2 nuclear accumulation without altering SMAD2 phosphorylation. (A) Western blot analysis for SMAD2, EEA1 (cytoplasmic marker), and LAMIN A/C (nuclear marker) in cytoplasmic (C) and nuclear (N) fractions extracted from CdCl₂-induced SKOV3-Ve1 and -M cells treated with or without 25 pM TGF- β . Lysates were collected at 0.5, 1, and 4 h after TGF- β treatment. The line graph shows quantification of the immunoblot expressed as the ratio of nuclear to total (C+N) SMAD2 for TGF- β -treated cells. The histogram summarizes three independent experiments (mean \pm SEM) examining SMAD2 subcellular localization after treatment with TGF- β for 1 h. Data are expressed as the ratio of nuclear to total SMAD2 relative to that measured in TGF- β -treated SKOV3-M cells (set to 1.0). Bars with different letters are statistically different from one another as determined by ANOVA followed by SNK post hoc test ($P < 0.05$). (B) VEPH1 knockdown enhances TGF- β -induced SMAD2 and SMAD3 nuclear accumulation in ES2 cells. A representative of three independent Western blots for SMAD2, SMAD3, EEA1, and Fibrillarin (nuclear marker) in C and N fractions extracted from siLuc- or siVEPH1-transfected ES2 cells treated with or without 100 pM TGF- β . ES2 cells were transfected 72 h before treatment with TGF- β , and lysates were collected after 0.5 and 2 h. The line graph shows quantification of the immunoblots expressed as the ratio of nuclear to total (C + N) SMAD2 or nuclear SMAD3 to Fibrillarin. The Western blot *inset* in the line graph shows VEPH1 expression levels in siLuc- or siVEPH1-transfected ES2 cells. (C) A representative of three independent Western blots showing equivalent TGF- β -induced C-terminal phosphorylated SMAD2 levels in SKOV3-M and -Ve1 cells. CdCl₂-induced SKOV3-Ve1 and -M cells were treated with or without 25 pM TGF- β for the times indicated.

whereas a weak interaction was detected with $\Delta 91$ (Fig. 7E). An interaction with T β RI was not detected with 90 Δ – $\Delta 201$. Furthermore, both 200 Δ – $\Delta 320$ and $\Delta 91$ inhibited TGF- β signaling, whereas 90 Δ – $\Delta 201$ had no impact (Fig. 7F). Collectively, these findings demonstrate that the ability of VEPH1 fragments to modulate TGF- β signaling associates with their ability to interact with T β RI.

Increased SMAD2–T β RI Interaction by Truncated VEPH1 Proteins Correlates with Their Inhibition of TGF- β Signaling. Our results indicate that TIR-1 activity is essential for an inhibitory impact of VEPH1 on TGF- β signaling, whereas TIR-2 facilitates TGF- β signaling in the absence of TIR-1. We therefore compared the impact of TIR-1-containing $\Delta 661$ and 662 Δ (TIR-2) on SMAD2 association with T β RI using semiquantitative LUMIER. Full-length VEPH1 stabilized SMAD2 interaction with both WT and TD T β RI (Fig. 8A), similar to our analysis above (Fig. 6D). Whereas $\Delta 661$ further enhanced these interactions, 662 Δ destabilized SMAD2 association with T β RI, compared with empty-vector-transfected cells (Fig. 8A). Thus, the ability of full-length and truncated VEPH1 proteins to modulate the stability of the SMAD2–T β RI interaction correlates with their inhibitory or stimulatory effect on TGF- β signaling.

To further verify that VEPH1 inhibition of TGF- β signaling is independent of T β RI kinase activity, COS7 cells were transfected

with TD T β RI and either full-length VEPH1, $\Delta 661$, or 662 Δ , and their impact on SMAD2-dependent pARE-luciferase activation was determined in the presence or absence of TGF- β . As expected, TGF- β treatment resulted in increased luciferase activity due to its activation of endogenous WT T β RI. Both full-length VEPH1 and $\Delta 661$ inhibited, whereas 662 Δ enhanced, pARE-luciferase activity in nontreated, as well as TGF- β -treated, cells relative to controls (Fig. 8B). These findings indicate that both the inhibitory effects of VEPH1 and the enhancing effects of TIR-2 are downstream of T β RI kinase activation and are consistent with VEPH1 acting to modulate SMAD2 dissociation from T β RI.

To further investigate TIR-2 activities, its impact on SMAD2 nuclear localization and phosphorylation were examined in cells stably expressing EGFP-tagged 662 Δ or EGFP alone as a control. Stable expression of EGFP-662 Δ was verified by Western blot analysis (Fig. 8C). Treatment of cells with TGF- β for 1 h increased nuclear SMAD2, which returned to near baseline by 2 h after treatment (Fig. 8D). Expression of 662 Δ enhanced TGF- β -induced SMAD2 nuclear accumulation and prolonged its retention. To determine whether these changes were associated with altered C-terminal phosphorylation of SMAD2, we compared levels of phospho-SMAD2 in 662 Δ or control cells. Time-course analysis indicated elevated TGF- β -induced phospho-SMAD2 levels at all time points in 662 Δ -expressing cells compared with

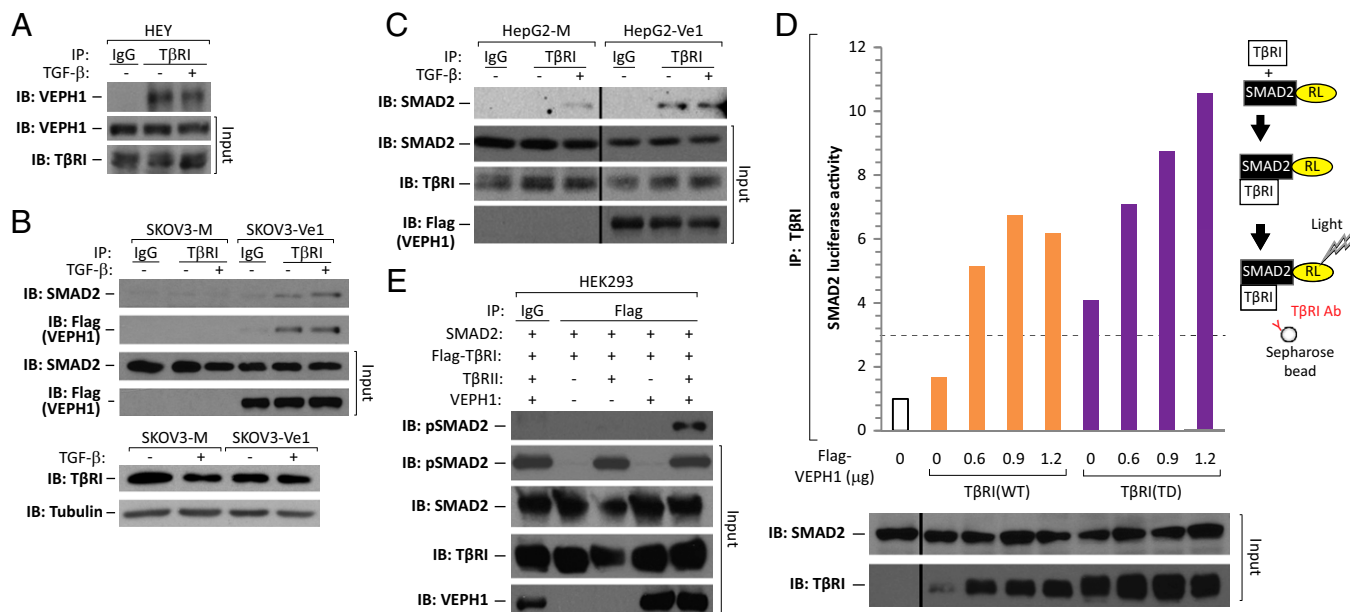


Fig. 6. VEPH1 interacts with T β RI and promotes retention of SMAD2 at T β RI. (A) Coimmunoprecipitation of endogenous T β RI with VEPH1 in HEY cells treated with or without 200 pM TGF- β for 1 h. (B) Coimmunoprecipitation of T β RI with VEPH1 and with SMAD2 in SKOV3-Ve1 cells. Induced SKOV3-Ve1 and -M cells were treated with or without 200 pM TGF- β for 1 h. Lysates immunoprecipitated with nonimmune IgG were used as a control. T β RI levels shown were determined in the cell lines in a separate experiment. (C) Coimmunoprecipitation of T β RI with SMAD2 in HepG2-Ve1 and -M cells. CdCl₂-induced HepG2 stable cells were treated with or without 200 pM TGF- β for 0.5 h. Lysates immunoprecipitated with nonimmune IgG were used as a control. (D) Semiquantitative LUMIER assay showing increased SMAD2-T β RI interaction in the presence of VEPH1. HEK293T cells were transiently transfected with expression constructs for WT or TD T β RI and RL-tagged SMAD2 in the presence or absence of increasing amounts of VEPH1. Cell lysates were immunoprecipitated with an anti-T β RI antibody, and the resulting precipitates were assessed for RL activity. The dashed line represents the minimum value reflecting a significant interaction (37). RL-SMAD2 and T β RI levels in total lysates before immunoprecipitation (input) are shown by Western blot. (E) VEPH1 promotes T β RI retention of phosphorylated SMAD2. HEK293T cells were transiently transfected with expression constructs for WT T β RI and SMAD2, in the presence or absence of T β RII and VEPH1. Lysates immunoprecipitated with nonimmune IgG were used as a control. IB, immunoblotting antibody; input, nonimmunoprecipitated lysates; IP, immunoprecipitating antibody.

control cells (Fig. 8E). Maximal phospho-SMAD2 was detected at 1 h after treatment with TGF- β and began to decrease by 2 h. Thus, 662 Δ functions to enhance C-terminal SMAD2 phosphorylation, leading to its increased nuclear accumulation.

Discussion

Studies with *meteld* mutant flies indicate important developmental effects, mediated at least in part by modulation of the FOXO and Hippo signaling pathways. Our gene-expression data generated with SKOV3 ovarian cancer cells indicate human VEPH1 also impacts these signaling systems and additionally the Wnt and TGF- β signaling pathways. We demonstrate a unique inhibitory role for VEPH1 on SMAD2/3-dependent TGF- β signaling. Our findings indicate that VEPH1 is a membrane-localized T β RI-interacting protein that retains SMAD2 at T β RI, without affecting SMAD2 C-terminal phosphorylation. This hindered release correlates with diminished SMAD2 nuclear accumulation and negative modulation of SMAD2/3-dependent TGF- β target genes.

The binding, phosphorylation, and release of SMAD2/3 from T β RI is highly coordinated, involving multiple partnering proteins, such as FKBP12 (FK506-binding protein 1A, 12 kDa) and SARA (SMAD anchor for receptor activation) (reviewed in ref. 40). Inactive T β RI is bound to inhibitory protein FKBP12. In response to TGF- β binding, T β RII forms a stable complex with, and transphosphorylates, T β RI. The resulting conformational change dissociates FKBP12, enhancing T β RI binding to SMAD2/3 (41). SARA interacts with and controls SMAD2/3 subcellular localization and recruitment to T β RI (40). VEPH1 expression resulted in SMAD2 interaction with T β RI, even in the absence of TGF- β stimulation. Although this result raises the possibility that VEPH1 could promote activation of T β RI to result in its asso-

ciation with SMAD2 in the absence of TGF β , we did not detect phospho-SMAD2 in the absence of TGF β treatment. Further studies are required to determine whether other proteins might be involved with the inhibitory role of VEPH1.

Knockdown of endogenous VEPH1 resulted in increased TGF- β -induced nuclear accumulation of SMAD2 and SMAD3. In contrast to SMAD2, the increase in SMAD3 may reflect increased SMAD3 stability induced by TGF- β (Fig. S4B). The Axin/GSK3- β complex promotes proteasome-dependent degradation of SMAD3, but not SMAD2, in the absence of TGF- β signaling (42). Although VEPH1 could impair SMAD3 nuclear accumulation through a mechanism similar to SMAD2, it is also possible that VEPH1 could affect the Axin/GSK3- β complex to enhance SMAD3 degradation.

The VEPH1 N-terminal and PH-domain-containing regions that interact with T β RI have opposing impacts on TGF- β signaling that is reflected in their ability to sequester SMAD2 at T β RI. Whereas the N-terminal region (TIR-1) inhibits signaling similar to the full-length protein and promotes SMAD2 retention at T β RI, the isolated PH-domain-containing region (TIR-2) enhances signaling and promotes dissociation of SMAD2 from T β RI, resulting in elevated nuclear SMAD2 accumulation. These findings indicate that the TIR-1 region of VEPH1 is crucial for the inhibitory effect of the full-length protein. Our data further indicate that there are two subregions within TIR-1 that interact with T β RI and independently inhibit TGF- β signaling; however, a more pronounced inhibition is obtained with an intact TIR-1.

The enhancing effect of TIR-2 was also observed in HEY cells, suggesting that this truncated protein opposes endogenous VEPH1 activity. Of interest, murine Veph1 isoform B (Veph-B; GenBank accession no. BAC02922) is predicted to encode a truncated 253-amino-acid protein corresponding to the PH-domain-containing

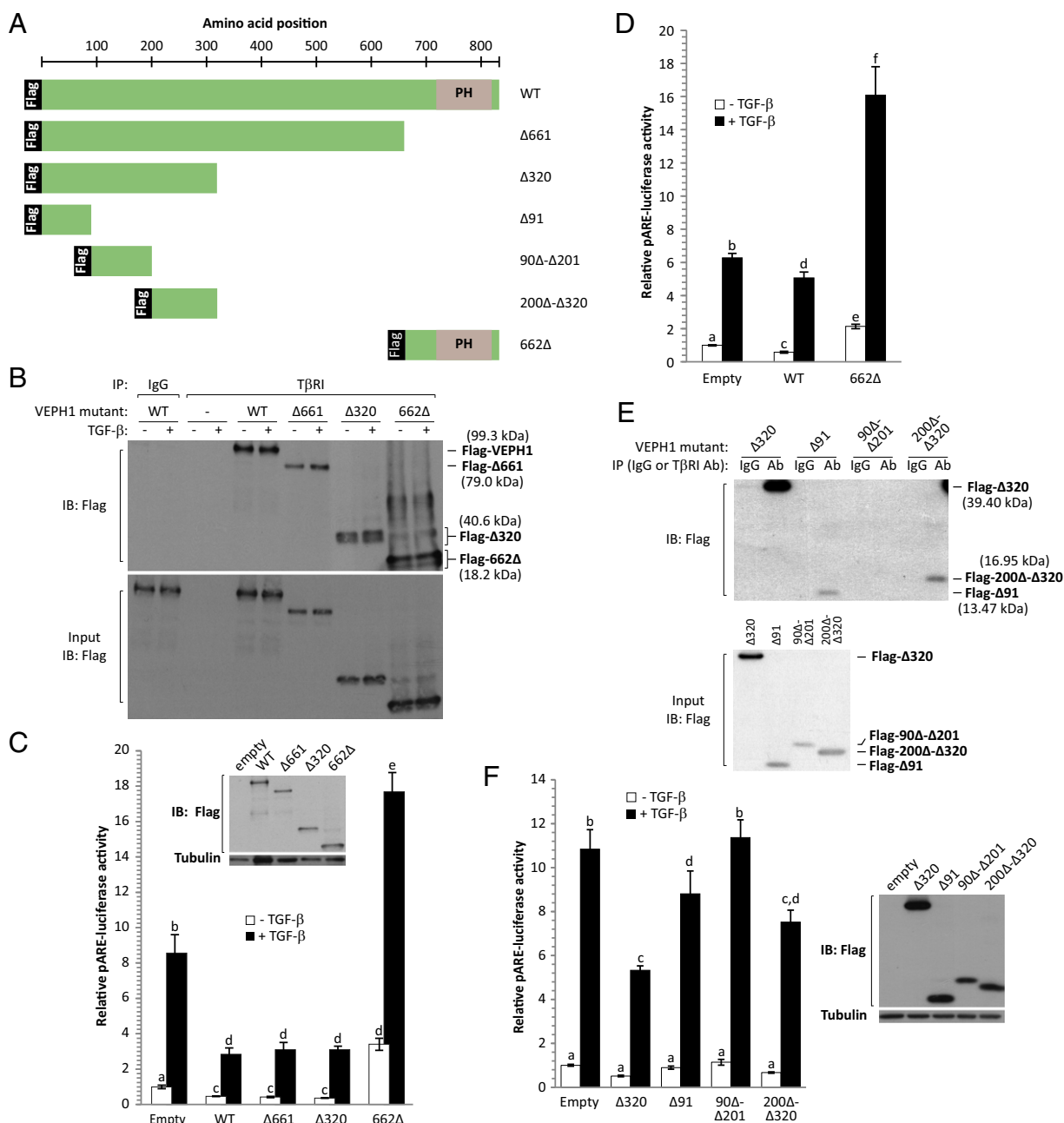


Fig. 7. VEPH1 inhibition of TGF- β signaling is dependent on its interaction with T β RI. (A) Schematic showing Flag-tagged VEPH1 fragments generated by site-directed mutagenesis and cloning. WT, full-length VEPH1; Δ 661, p.M661X; Δ 320, p.E320X; 662 Δ , p.M1_M662del., amino acids 1–90 (Δ 91); 91–200 (90 Δ – Δ 201); and 201–319 (200 Δ – Δ 320). PH, pleckstrin homology domain. (B) VEPH1 N- and C-terminal regions interact with T β RI independent of TGF- β . Lysates were collected after 1-h treatment with TGF- β and immunoprecipitated with anti-T β RI antibody or control IgG. (C) N- and C-terminal regions of VEPH1 inhibit and enhance TGF- β signaling, respectively. COS7 cells transiently transfected with empty expression vector or truncated Flag-VEPH1 expression constructs and pARE-luciferase were treated with or without 100 pM TGF- β for 24 h. *Inset* shows levels of Flag immunoreactivity indicative of full-length or truncated VEPH1 expression. (D) The C-terminal PH domain-containing region of VEPH1 (662 Δ) enhances TGF- β signaling in HEY cells. Cells were transiently transfected with VEPH1 expression constructs or empty vector and pARE-luciferase reporter and treated with or without 100 pM TGF- β for 24 h. (E) Determination of T β RI-binding regions within the VEPH1 N-terminal region. Lysates from COS7 cells transfected with VEPH1 expression constructs were immunoprecipitated with an anti-T β RI antibody or control IgG. (F) Inhibition of TGF- β signaling by VEPH1 N-terminal fragments shown to interact with T β RI. COS7 cells transfected with expression constructs for N-terminal region VEPH1 and pARE-luciferase were treated with or without 100 pM TGF- β for 24 h. *Right* shows levels of Flag immunoreactivity indicative of truncated VEPH1 expression. For all reporter assays, firefly luciferase activity was normalized to RL activity. For pARE-luciferase assays, cells were cotransfected with a FoxH1 expression construct. Bars represent mean \pm SEM, $n = 3$. Bars with different letters are statistically different from one another as determined by ANOVA followed by SNK post hoc test ($P < 0.05$). IB, immunoblotting antibody; input, nonimmunoprecipitated lysates; IP, immunoprecipitating antibody.

region. Thus, expression of the isolated TIR-2 region of Veph1, as well as full-length Veph1 (Veph-A; GenBank accession no. BAC02920), may have opposing effects on TGF- β signaling. Both

the VEPH1 N-terminal and PH domain regions are well conserved, and protein domain analysis using the database of ELM (32) predicts multiple protein interaction motifs within these regions.

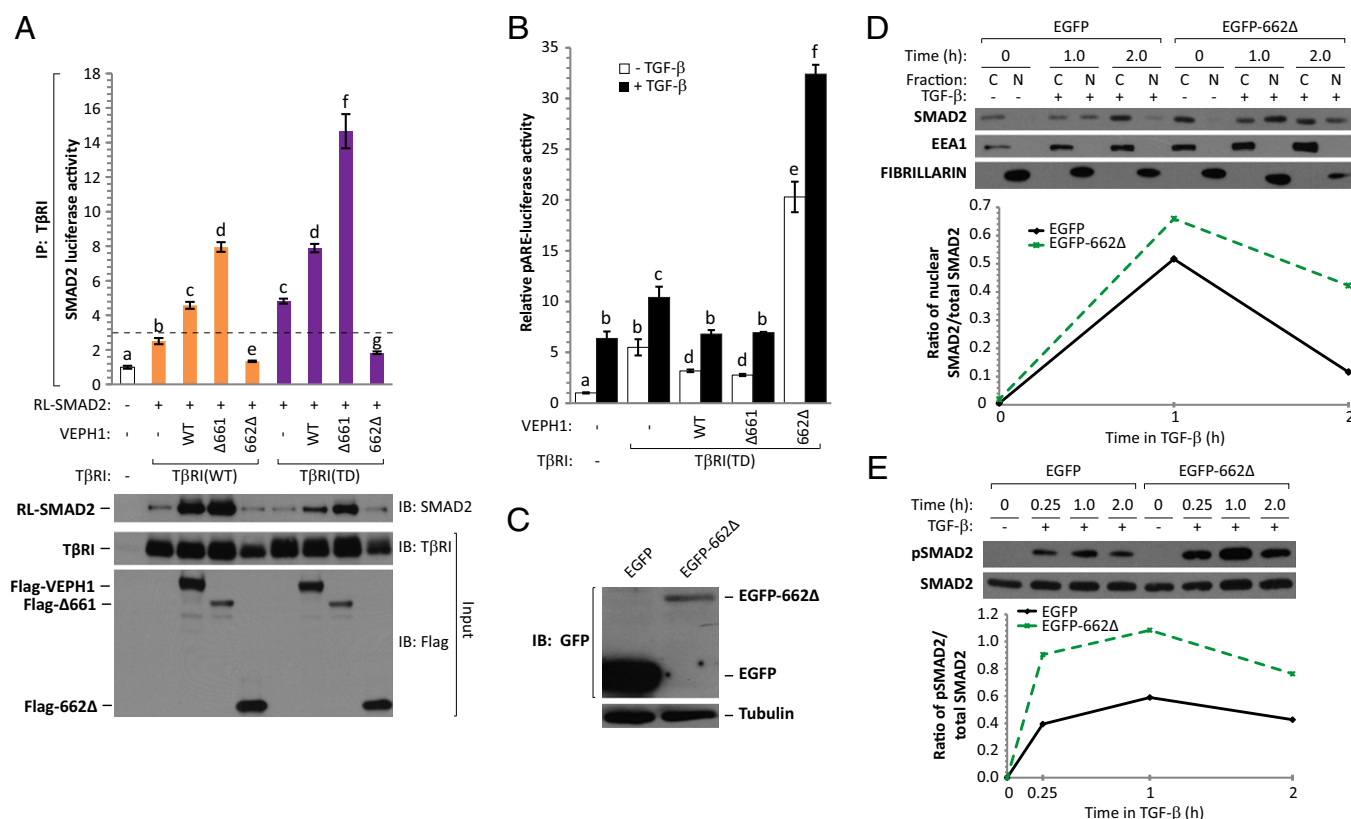


Fig. 8. Increased SMAD2-TβRI interaction by truncated VEPH1 proteins correlates with their negative impact on TGF-β signaling. (A) Semiquantitative LUMIER assay showing enhanced SMAD2-TβRI interaction in the presence of TGF-β inhibiting VEPH1 truncated proteins. HEK293T cells were transfected with WT or TD TβRI and RL-tagged SMAD2 expression constructs in the presence or absence of WT, Δ661, or 662Δ VEPH1. Cell lysates were immunoprecipitated with an anti-TβRI antibody, and the resulting precipitates were assessed for RL activity. The dashed line represents the minimum value reflecting a significant interaction (37). Immunoblotting for RL-SMAD2 was performed on immunoprecipitates. TβRI and Flag-VEPH1 protein levels in total lysates before immunoprecipitation (input) are shown by Western blot. IB, immunoblotting antibody; IP, immunoprecipitating antibody. (B) VEPH1 inhibits TGF-β signaling downstream of TβRI activation. COS7 cells transfected with TβRI(TD), pARE-luciferase, and expression constructs for full-length or truncated VEPH1 were treated with or without 100 pM TGF-β for 24 h. Bars represent the mean ± SEM, *n* = 3. Bars with different letters are statistically different from one another as determined by ANOVA followed by SNK post hoc test (*P* < 0.05). (C) GFP immunoblot showing EGFP or EGFP-662Δ expression in stably transfected COS7 cells. (D and E) 662Δ enhances TGF-β-dependent SMAD2 nuclear accumulation and C-terminal phosphorylation. (D) Western blot analysis for SMAD2, EEA1 (cytoplasmic marker), and Fibrillarlin (nuclear marker) in cytoplasmic (C) and nuclear (N) fractions extracted from EGFP-662Δ or EGFP stable COS7 cells treated with or without 100 pM TGF-β. Lysates were collected at 1 and 2 h after TGF-β treatment. The line graph shows quantification of the immunoblot expressed as the ratio of nuclear to total (C+N) SMAD2. (E) Western blot of C-terminal phosphorylated and total SMAD2 levels in stable EGFP or EGFP-662Δ COS7 cells treated with or without 100 pM TGF-β for 0.25, 1, or 2 h. The line graph shows quantification of the immunoblot expressed as the ratio of phosphorylated to total SMAD2.

Future studies will define whether these motifs are critical for the observed divergent effects of TIR-1 and -2 on TGF-β signaling.

Teleman et al. (2) reported that deletion of *Melted* in *Drosophila* led to a “reprogramming” of cells within the fat body, affecting the expression of genes involved in fatty acid metabolism and immune function. Pathway analysis of our expression data also indicates altered expression of genes involved in metabolism, phototransduction, and immune response, suggesting conservation of function between VEPH1 and Melted. Although Melted has been shown to affect Hippo, FOXO, and TOR signaling pathways, TGF-β is also involved with vertebrate adipocyte differentiation (43) and eye development (44). VEPH1 regions containing TIR-1 and -2 have 44% and 42% sequence identity and 65% and 62% positivity, respectively, with Melted. Thus, future studies should explore the impact of VEPH1 on cell-signaling pathways affected by Melted. Our findings also raise the possibility that some effects of Melted may be mediated through an impact on signaling by *Drosophila* TGF-β superfamily members. Collectively, the evidence support that Melted and VEPH1 may function as membrane scaffolding proteins to integrate and modulate these signaling pathways.

Although some studies suggest that the dysregulation of TGF-β signaling in ovarian cancer is due to *TβRI* or *TβRII* gene mu-

tations or reduced SMAD4 expression (45–48), other studies have reported that alterations in TGF-β signaling are independent of TGF-β receptors or downstream SMADs. In recent studies, altered expression of known TGF-β signaling regulators (49) and epigenetic silencing of TGF-β target genes in ovarian cancer (50–52) have been reported. The present study identifies VEPH1 as a unique negative modulator of canonical TGF-β signaling.

The gene encoding VEPH1 localizes to a region frequently reported as amplified in ovarian cancer (8, 9). Microarray comparative genomic hybridization analysis indicated amplification of the 3q24-26 region in 7 of 12 ovarian clear cell carcinoma cell lines examined, including ES2 cells (8). In addition to ES2 cells, we found high levels of VEPH1 expression in OVCA429 and HEY cells, which were derived from serous adenocarcinomas. Whether the *VEPH1* locus is amplified in these cells is unknown. These three cell lines exhibit a more invasive phenotype than OVCAR3, SKOV3, and HOC7 cells (53), which lack VEPH1 expression, raising the possibility that VEPH1 may contribute to a more aggressive cell phenotype or to the initiation of a subset of ovarian cancers.

In summary, studies with *Drosophila* indicate that Melted impacts several signal-transduction pathways during development that overlap with those we show are affected by VEPH1 expression. We now demonstrate that VEPH1 is a previously unidentified

modulator of the canonical TGF- β signaling pathway and acts to restrict SMAD2 nuclear accumulation through retention of SMAD2 at T β RI. Because VEPH1 is up-regulated in many ovarian cancers and is highly expressed in invasive ovarian cancer cell lines, these findings suggest that VEPH1 may contribute to carcinogenesis by blocking canonical TGF- β signaling.

Materials and Methods

A detailed outline of the procedures and specific materials used for cell culture; generation of expression constructs and stably transfected SKOV3, HepG2, and COS7 cells; gene expression profiling and analysis; quantitative RT-PCR (RT-qPCR); Western blot analysis; VEPH1-targeted siRNA studies; immunofluorescence microscopy; reporter gene assays; coimmunoprecipitation assays;

and statistical analysis are provided in *SI Materials and Methods*. Gene-expression profiles were generated by using the Illumina Human HT-12 Bead-Chip platform (Version 4.0). A corrected (Benjamini-Hochberg; false discovery rate < 0.05) ANOVA followed by a Tukey post hoc test was performed to identify probes whose mean expression was significantly different between treatment groups. Microarray data have been deposited into the Gene Expression Omnibus database (accession no. GSE67765).

ACKNOWLEDGMENTS. We thank Drs. Miriam Barrios-Rodiles and Xaralabos Varelas for technical advice; Drs. Veronique Voisin and Gary Bader for assistance with GSEA and Cytoscape analysis; and Soyeon Park for technical assistance. This work was supported by Canadian Institutes of Health Research Grant MOP74726. P.S. was supported in part by a Kristi Piia Callum Memorial Fellowship, a Frank Fletcher Memorial Fund, and a Teresina Florio Graduate Scholarship.

- Muto E, et al. (2004) Identification and characterization of Veph, a novel gene encoding a PH domain-containing protein expressed in the developing central nervous system of vertebrates. *Biochimie* 86(8):523–531.
- Teleman AA, Chen YW, Cohen SM (2005) Drosophila Melted modulates FOXO and TOR activity. *Dev Cell* 9(2):271–281.
- Mikeladze-Dvali T, et al. (2005) The growth regulators warts/lats and melted interact in a bistable loop to specify opposite fates in Drosophila R8 photoreceptors. *Cell* 122(5):775–787.
- Jukam D, Desplan C (2011) Binary regulation of Hippo pathway by Merlin/NF2, Kibra, Lgl, and Melted specifies and maintains postmitotic neuronal fate. *Dev Cell* 21(5):874–887.
- Jukam D, et al. (2013) Opposite feedbacks in the Hippo pathway for growth control and neural fate. *Science* 342(6155):1238016.
- Iwabuchi H, et al. (1995) Genetic analysis of benign, low-grade, and high-grade ovarian tumors. *Cancer Res* 55(24):6172–6180.
- Haverty PM, Hon LS, Kaminker JS, Chant J, Zhang Z (2009) High-resolution analysis of copy number alterations and associated expression changes in ovarian tumors. *BMC Med Genomics* 2:21.
- Tan DS, et al. (2009) PPM1D is a potential therapeutic target in ovarian clear cell carcinomas. *Clin Cancer Res* 15(7):2269–2280.
- Ramakrishna M, et al. (2010) Identification of candidate growth promoting genes in ovarian cancer through integrated copy number and expression analysis. *PLoS ONE* 5(4):e9983.
- Schmierer B, Hill CS (2007) TGF β -SMAD signal transduction: molecular specificity and functional flexibility. *Nat Rev Mol Cell Biol* 8(12):970–982.
- Shi Y, Massagué J (2003) Mechanisms of TGF- β signaling from cell membrane to the nucleus. *Cell* 113(6):685–700.
- Akhurst RJ, Derynck R (2001) TGF- β signaling in cancer—a double-edged sword. *Trends Cell Biol* 11(11):544–551.
- Massagué J (2008) TGF β in Cancer. *Cell* 134(2):215–230.
- Siegel PM, Massagué J (2003) Cytostatic and apoptotic actions of TGF- β in homeostasis and cancer. *Nat Rev Cancer* 3(11):807–821.
- Massagué J, Gomis RR (2006) The logic of TGF β signaling. *FEBS Lett* 580(12):2811–2820.
- Pardali K, Moustakas A (2007) Actions of TGF- β as tumor suppressor and prometastatic factor in human cancer. *Biochim Biophys Acta* 1775(1):21–62.
- Wang YQ, Qi XW, Wang F, Jiang J, Guo QN (2012) Association between TGFBR1 polymorphisms and cancer risk: A meta-analysis of 35 case-control studies. *PLoS ONE* 7(8):e42899.
- Taylor BS, et al. (2010) Integrative genomic profiling of human prostate cancer. *Cancer Cell* 18(1):11–22.
- Imielinski M, et al. (2012) Mapping the hallmarks of lung adenocarcinoma with massively parallel sequencing. *Cell* 150(6):1107–1120.
- Brennan CW, et al.; TCGA Research Network (2013) The somatic genomic landscape of glioblastoma. *Cell* 155(2):462–477.
- Koboldt DC, et al.; Cancer Genome Atlas Network (2012) Comprehensive molecular portraits of human breast tumours. *Nature* 490(7418):61–70.
- Baca SC, et al. (2013) Punctuated evolution of prostate cancer genomes. *Cell* 153(3):666–677.
- Barretina J, et al. (2010) Subtype-specific genomic alterations define new targets for soft-tissue sarcoma therapy. *Nat Genet* 42(8):715–721.
- Cancer Genome Atlas Research Network (2014) Comprehensive molecular characterization of urothelial bladder carcinoma. *Nature* 507(7492):315–322.
- Kandoth C, et al.; Cancer Genome Atlas Research Network (2013) Integrated genomic characterization of endometrial carcinoma. *Nature* 497(7447):67–73.
- Bell D, et al.; Cancer Genome Atlas Research Network (2011) Integrated genomic analyses of ovarian carcinoma. *Nature* 474(7353):609–615.
- Barretina J, et al. (2012) The Cancer Cell Line Encyclopedia enables predictive modelling of anticancer drug sensitivity. *Nature* 483(7391):603–607.
- Grasso CS, et al. (2012) The mutational landscape of lethal castration-resistant prostate cancer. *Nature* 487(7406):239–243.
- Hammerman PS, et al.; Cancer Genome Atlas Research Network (2012) Comprehensive genomic characterization of squamous cell lung cancers. *Nature* 489(7417):519–525.
- Subramanian A, et al. (2005) Gene set enrichment analysis: A knowledge-based approach for interpreting genome-wide expression profiles. *Proc Natl Acad Sci USA* 102(43):15545–15550.
- Mootha VK, et al. (2003) PGC-1 α -responsive genes involved in oxidative phosphorylation are coordinately downregulated in human diabetes. *Nat Genet* 34(3):267–273.
- Dinkel H, et al. (2012) ELM—the database of eukaryotic linear motifs. *Nucleic Acids Res* 40(Database issue):D242–D251.
- Ilzecka J, Stelmasiak Z, Dobosz B (2002) Transforming growth factor-Beta 1 (tgf-Beta 1) in patients with amyotrophic lateral sclerosis. *Cytokine* 20(5):239–243.
- Kriegstein K, Unsicker K (1996) Distinct modulatory actions of TGF- β and LIF on neurotrophin-mediated survival of developing sensory neurons. *Neurochem Res* 21(7):843–850.
- Walsh JE, Young MR (2011) TGF- β regulation of focal adhesion proteins and motility of premalignant oral lesions via protein phosphatase 1. *Anticancer Res* 31(10):3159–3164.
- Cicchini C, et al. (2008) TGF β -induced EMT requires focal adhesion kinase (FAK) signaling. *Exp Cell Res* 314(1):143–152.
- Barrios-Rodiles M, et al. (2005) High-throughput mapping of a dynamic signaling network in mammalian cells. *Science* 307(5715):1621–1625.
- Zawel L, et al. (1998) Human Smad3 and Smad4 are sequence-specific transcription activators. *Mol Cell* 1(4):611–617.
- Labbé E, Silvestri C, Hoodless PA, Wrana JL, Attisano L (1998) Smad2 and Smad3 positively and negatively regulate TGF β -dependent transcription through the forkhead DNA-binding protein FAST2. *Mol Cell* 2(1):109–120.
- Massagué J, Chen YG (2000) Controlling TGF- β signaling. *Genes Dev* 14(6):627–644.
- Huse M, et al. (2001) The TGF β receptor activation process: An inhibitor- to substrate-binding switch. *Mol Cell* 8(3):671–682.
- Guo X, et al. (2008) Axin and GSK3- control Smad3 protein stability and modulate TGF- signaling. *Genes Dev* 22(1):106–120.
- Lu H, Ward MG, Adeola O, Ajuwon KM (2013) Regulation of adipocyte differentiation and gene expression-crosstalk between TGF β and wnt signaling pathways. *Mol Biol Rep* 40(9):5237–5245.
- Grocott T, Johnson S, Bailey AP, Streit A (2011) Neural crest cells organize the eye via TGF- β and canonical Wnt signalling. *Nat Commun* 2:265.
- Antony ML, Nair R, Sebastian P, Karunakaran D (2010) Changes in expression, and/or mutations in TGF- β receptors (TGF- β RI and TGF- β RII) and Smad 4 in human ovarian tumors. *J Cancer Res Clin Oncol* 136(3):351–361.
- Lynch MA, et al. (1998) Mutational analysis of the transforming growth factor beta receptor type II gene in human ovarian carcinoma. *Cancer Res* 58(19):4227–4232.
- Wang D, et al. (2000) Analysis of specific gene mutations in the transforming growth factor- β signal transduction pathway in human ovarian cancer. *Cancer Res* 60(16):4507–4512.
- Chen T, et al. (2001) Transforming growth factor-beta receptor type I gene is frequently mutated in ovarian carcinomas. *Cancer Res* 61(12):4679–4682.
- Sunde JS, et al. (2006) Expression profiling identifies altered expression of genes that contribute to the inhibition of transforming growth factor-beta signaling in ovarian cancer. *Cancer Res* 66(17):8404–8412.
- Chou JL, Chen LY, Lai HC, Chan MW (2010) TGF- β : Friend or foe? The role of TGF- β /SMAD signaling in epigenetic silencing of ovarian cancer and its implication in epigenetic therapy. *Expert Opin Ther Targets* 14(11):1213–1223.
- Chou JL, et al. (2010) Promoter hypermethylation of FBXO32, a novel TGF- β /SMAD4 target gene and tumor suppressor, is associated with poor prognosis in human ovarian cancer. *Lab Invest* 90(3):414–425.
- Chan MW, et al. (2008) Aberrant transforming growth factor beta1 signaling and SMAD4 nuclear translocation confer epigenetic repression of ADAM19 in ovarian cancer. *Neoplasia* 10(9):908–919.
- Sodek KL, Ringuette MJ, Brown TJ (2007) MT1-MMP is the critical determinant of matrix degradation and invasion by ovarian cancer cells. *Br J Cancer* 97(3):358–367.